Published in final edited form as:
J Cereb Blood Flow Metab. 2009 March ; 29(3): 524–533. doi:10.1038/jcbfm.2008.142.

uPA modulates the age-dependent effect of brain injury on cerebral hemodynamics through LRP and ERK MAPK

William M Armstead[1,2], **Douglas B Cines**[3], **Khalil H Bdeir**[3], **Yasmina Bdeir**[3], **Sherman C Stein**[4], and **Abd Al-Roof Higazi**[3,5]

[1]Department of Anesthesiology and Critical Care, University of Pennsylvania, Philadelphia, Pennsylvania, USA

[2]Department of Pharmacology, University of Pennsylvania, Philadelphia, Pennsylvania, USA

[3]Laboratory Medicine, Department of Pathology, University of Pennsylvania, Philadelphia, Pennsylvania, USA

[4]Department of Neurosurgery, University of Pennsylvania, Philadelphia, Pennsylvania, USA

[5]Department of Clinical Biochemistry, Hadassah Medical School, Hebrew University, Jerusalem, Israel

Abstract

We hypothesized that urokinase plasminogen activator (uPA) contributes to age-dependent early hyperemia after fluid percussion brain injury (FPI) by activating extracellular signal-related kinase (ERK) mitogen-activated protein kinase (MAPK), leading to histopathologic changes in the underlying cortex. Both cerebrospinal fluid (CSF) uPA and phosphorylation of CSF ERK MAPK was increased at 1 min after FPI in newborn pigs, but was unchanged in juvenile pigs. uPA and phosphorylated ERK MAPK, detectable in sham piglet brain by immunohistochemistry, was markedly elevated and associated with histopathology 4 h after FPI in the newborn but there was minimal staining and histopathology in the juvenile. EEIIMD, a peptide derived from PA inhibitor-1 that does not affect proteolysis, blunted FPI-induced phosphorylation of ERK MAPK. FPI produced pial artery dilation and increased cerebral blood flow at 1 min after insult in the newborn, but not in the juvenile. Antilipoprotein-related protein (LRP) antibody, EEIIMD, a soluble uPA antagonist, and the ERK MAPK antagonist U 0126 inhibited FPI-associated hyperemia. These data indicate that uPA is upregulated after FPI and produces an age-dependent early hyperemia followed by histopathology through an LRP- and ERK MAPK-dependent pathway.

Keywords

cerebral circulation; newborn; plasminogen activators; signal transduction

Correspondence: Dr WM Armstead, Department of Anesthesiology and Critical Care, University of Pennsylvania, 3620 Hamilton Walk, JM3, Philadelphia, PA l9l04, USA. armsteaw@uphs.upenn.edu.

Disclosure/conflict of interest
The authors have no duality of interest to declare.

Introduction

Traumatic brain injury (TBI) is the most common cause of brain injury and the leading cause of death and disability in children (Rodriguez, 1990). Although the effects of TBI have been extensively investigated in models involving adult animals (Wei *et al*, 1980), less is known about TBI in the newborn/infant. TBI can cause uncoupling of blood flow and metabolism, resulting in cerebral ischemia or hyperemia (Richards *et al*, 2001). Although cerebral hyperemia was historically considered the cause of diffuse brain swelling after TBI in the pediatric setting (Bruce *et al*, 1981), recent evidence suggests that cerebral hypoperfusion is the dominant derangement (Adelson *et al*, 1997*a*). Decreases in cerebral blood flow (CBF) and pial artery diameter, along with impaired vasodilator responsiveness are greater in newborn than in juvenile pigs after fluid percussion brain injury (FPI) (Armstead and Kurth, 1994), a model of concussive head injury (Gennarelli, 1994). These data support the potential importance of hypoperfusion in outcome after TBI and the concept that the cerebral hemodynamics in the newborn is more sensitive to brain injury (Armstead and Kurth, 1994). However, a more harmonious interpretation of the literature involving pediatric TBI might include the possible coexistence of both hyper- and hypoperfusion after TBI, the relative importance of which varies as a function of age and time after insult. Piglets offer the unique advantage in elucidating these pathways by virtue of having a gyrencepahalic brain that contains substantial white matter, which is more sensitive to ischemic/TBI damage than grey matter, similar to humans.

Recent studies suggest the plasminogen activator system is involved in the development of post-TBI injury. Urokinase and tissue plasminogen activator (uPA and tPA) are serine proteases that convert plasminogen to the active protease plasmin (Collen and Lijnen, 1991). Our studies show that exogenous uPA produces pial artery dilation in the pig (Armstead *et al*, 2005). The effect of plasminogen activators (PAs) on vascular activity is mediated through the low-density lipoprotein receptor (LRP; Bu *et al*, 1992). EEIIMD, a peptide derived from the endogenous PA inhibitor PAI-1, and soluble urokinase plasminogen activator receptor (suPAR) each inhibit PA-mediated vasodilation without compromising catalytic activity (Armstead *et al*, 2005; Nassar *et al*, 2004; Akkawi *et al*, 2006). The concentration of tPA in the CSF is elevated to a greater extent in the newborn than the juvenile pig within 1 h of FPI (Armstead *et al*, 2005). EEIIMD and suPAR blunt pial artery vasoconstriction observed at 1 h after injury in an age-dependent manner (Armstead *et al*, 2005), whereas EEIIMD blunted FPI-associated histopathology (Armstead *et al*, 2006). Global cerebral ischemia in the piglet exhibits an initial hyperemia within 5 mins after delayed cerebral hypoperfusion evident within 1 h after insult (Leffler *et al*, 1989). Because earlier time points after FPI have not been investigated to date, it has not been determined whether the cerebral hemodynamic profile after TBI in the newborn is similar to those described after global cerebral ischemia.

The early effects of TBI on cerebral hemodynamics may be mediated through changes in mitogen-activated protein kinases (MAPKs), a key intracellular signaling system. The MAPK system is a family of at least three kinases, extracellular signal-related kinase (ERK), p38, and c-Jun N-terminal kinase (JNK) (Laher and Zhang, 2001). TBI induces the expression of neurotrophin related mRNA and receptors (Hicks *et al*, 1999), which subsequently triggers downstream MAPK cascades (Otani *et al*, 2002) through interactions with high-affinity tyrosine kinase receptors (Bonni *et al*, 1999). The vasoreactivity of uPA is mediated through the low-density lipoprotein receptor (LRP) (Nassar *et al*, 2002). Upregulation of plasminogen activators contributes to age-dependent impairment of cerebrovasodilation in response to activation of the *N*-methyl-D-aspartate (NMDA) receptor after FPI (Armstead *et al*, 2005). Independent studies show that ERK MAPK activation contributes to blunted NMDA-mediated dilation after FPI (Armstead, 2003). Our previous

studies also show an age-dependent increase in cerebral oxygenation, monitored by near infrared spectroscopy, within 1 min of FPI in the newborn pig, suggestive of early hyperemia (Armstead and Kurth, 1994).

We hypothesized that uPA contributes to an early age-dependent hyperemia after FPI through activation of ERK MAPK that promotes histopathologic changes in the underlying cortex.

Materials and methods

Materials

Recombinant single chain urokinase (uPA) was expressed in S2 cells, purified by antibody affinity chromatography and characterized for affinity to the cellular and soluble urokinase receptor (suPAR), for plasminogen activator activity and for fibrinolytic activity in the presence and absence of suPAR, as described previously (Higazi *et al*, 1996*a*, *b*, 1998). uPA migrates as a homogeneous −50 kDa protein on SDS–polyacrylamide gel electrophoresis under reducing and non-reducing conditions.

Closed Cranial Window, Cerebral Blood Flow Determination, and Brain Injury Procedures

Newborn and juvenile pigs (1 to 5 days old and 3 to 4 weeks old, 1.2 to 1.6 and 6.2 to 7.8 kg, respectively) of either sex were studied. All protocols were approved by the Institutional Animal Care and Use Committee. Animals were sedated with isoflurane (1 to 2 MAC). Anesthesia was maintained with a-chloralose (30 to 50 mg/kg, supplemented with 5 mg/kg/h i.v.). A catheter was inserted into a femoral artery to monitor blood pressure and to sample for blood gas tensions and pH. Drugs to maintain anesthesia were administered through a second catheter placed in a femoral vein. The trachea was cannulated, and the animals were ventilated with room air. A heating pad was used to maintain the animals at 37°C to 39°C, monitored rectally.

A cranial window was placed in the parietal skull of these anesthetized animals. This window consisted of three parts: a stainless steel ring, a circular glass coverslip, and three ports consisting of 17-gauge hypodermic needles attached to three precut holes in the stainless steel ring. For placement, the dura was cut and retracted over the cut bone edge. The cranial window was placed in the opening and cemented in place with dental acrylic. The volume under the window was filled with a solution, similar to CSF, of the following composition (mmol/L): 3.0 KCl, 1.5 $MgCl_2$, 1.5 $CaCl_2$, 132 NaCl, 6.6 urea, 3.7 dextrose, and 24.6 $NaHCO_3$. This artificial CSF was warmed to 37°C and had the following chemistry: pH 7.33, p_{CO_2} 46 mmHg, and p_{O_2} 43 mmHg, which was similar to that of endogenous CSF. Pial arterial vessel diameter was measured with a microscope, a camera, a video output screen, and a video microscaler.

CBF was measured in the cerebral cortex using radioactively labeled microspheres. Briefly, a known amount of radioactivity in 15-μm microspheres (300,000 to 800,000 spheres) was injected into the left ventricle and the injection line flushed with 1 mL of saline. Withdrawal of reference blood samples was begun 15 secs before microsphere injection and continued for 2 mins after the injection. The reference withdrawal rate was 1.03 mL/min. After each experiment, the pig was sacrificed and the brain removed and weighed. CBF was determined by counting cerebral cortex brain tissue samples in a γ-counter. The energy from each nuclide was separated by differential spectroscopy. Aliquots of the actual microsphere solutions injected were used for overlap calculations. The count in each milliliter per minute of blood flow was determined by dividing the counts in the reference withdrawal by the rate of reference withdrawal. Thus blood flow can be calculated as $Q = C \times R \times \mathrm{CR}^{-1}$, where Q is brain blood flow (mL/min), C is counts per minute (c.p.m.) in the tissue sample, R is the rate

of withdrawal of reference blood sample (mL/min), and CR is the total counts in the reference blood sample. CBF so determined reflect flow to the cerebral cortex both ipsilateral and contralateral to the injury site.

Methods for brain FPI have been described previously (Wei *et al*, 1980). A device designed by the Medical College of Virginia was used. A small opening was made in the parietal skull contralateral to the cranial window. A metal shaft was sealed into the opening on top of intact dura. This shaft was connected to the transducer housing, which was in turn connected to the fluid percussion device. The device itself consisted of an acrylic plastic cylindrical reservoir 60 cm long, 4.5 cm in diameter, and 0.5 cm thick. One end of the device was connected to the transducer housing, whereas the other end had an acrylic plastic piston mounted on O-rings. The exposed end of the piston was covered with a rubber pad. The entire system was filled with 0.9% saline. The percussion device was supported by two brackets mounted on a platform. FPI was induced by striking the piston with a 4.8 kg pendulum. The intensity of the injury (1.9 to 2.3 atm with a constant duration of 19 to 23 ms) was controlled by varying the height from which the pendulum was allowed to fall. The pressure pulse of the injury was recorded on a storage oscilloscope triggered photoelectrically by the fall of the pendulum. The amplitude of the pressure pulse was used to determine the intensity of the injury.

Protocol

Two types of pial vessels, small arteries (resting diameter, 120 to 160 μm) and arterioles (resting diameter, 50 to 70 μm) were examined to determine whether segmental differences in the effects of FPI could be identified. Typically, 2 to 3 mL of artificial CSF were flushed through the window over a 30 secs period, and excess CSF was allowed to run off through one of the needle ports. For sample collection, 300 μL of the total cranial window volume of 500 μL was collected by slowly infusing artificial CSF into one side of the window and allowing the CSF to drip freely into a collection tube on the opposite side.

Seven experimental groups were studied (all $n = 6$): (1) sham control, (2) sham control treated with mouse immunoglobulin G (IgG; 10 μg/mL) (3) FPI, vehicle treated, (4) FPI treated with the plasminogen activator antagonist EEIIMD (1 mg/kg or 10^{-7} mol/L), (5) FPI treated with the soluble urokinase inhibitor suPAR (1 mg/kg or 10^{-7} mol/L), (6) FPI treated with an anti-LRP antibody (0.1 mg/kg or 10 μg/mL; American Diagnostica no. 3402 (Stamford, CT, USA), directed at the α-chain of α_2 M-R/LRP), and (7) FPI treated with the ERK MAPK inhibitor U 0126 (1 mg/kg or 10^{-6} mol/L; Sigma, St Louis, MO, USA). The vehicle for all agents was 0.9% saline, except for the MAPK inhibitor, which used dimethylsulfoxide (100 μL) diluted with 9.9 mL 0.9% saline. In sham control and FPI-vehicle animals, CBF and pial artery diameter was determined and CSF samples collected at 0 (before FPI), 1, 10, 60, and 240 mins in the presence of the vehicle. In drug-treated FPI animals, IgG, EEIIMD, suPAR, anti-LRP antibody (Ab), or U 0126 were administered 30 mins before FPI and the insult protocol followed as described above. CSF samples for ERK MAPK determination were also collected in animals given topical uPA (10^{-7} mol/L) 4 h after FPI to determine if exogenous plasminogen activator would further augment ERK MAPK in the CSF under insult conditions.

ELISA

Commercially available ELISA Kits were used to quantify CSF uPA (Diapharma, West Chester, OH, USA) and ERK MAPK (Assay Designs, Ann Arbor, MI, USA) concentration. Phosphorylated ERK MAPK enzyme values were normalized to total form and then expressed as percentage of the control condition.

Immunohistochemistry

At 4 h after FPI, the animal was sacrificed and 2 thin slices of parietal cortex were cut parallel to the brain surface. These slices were placed in 4% paraformaldehyde for 24 h at 4°C and then subjected to Paraffin sectioning. Paraffin sections of the parietal cortex from piglet brains after FPI and from uninjured sham control animals were unwaxed, incubated in 10 mmol/L sodium citrate buffer pH 6.0 inside a food steamer (subboiling temperature) for 10 mins to unmask the antigen, endogenous peroxidase was blocked with 0.3% H_2O_2, and stained with anti-human uPA monoclonal antibody (5 μg/mL) (no. 3689; American Diagnostica), anti-Phospho-p44/42 MAPK rabbit monoclonal antibody which recognize the phosphorylated forms of both p42 and p44 kinases (ERK1 and ERK2) (1 μg/mL; Cell Signaling no. 4376, Billerica, MA, USA), or with mouse IgG_1 as a negative control, secondary biotinylated antimouse IgG (1:200), followed by incubation with horse-radish peroxidase-conjugated streptavidin. Peroxidase was detected using the avidin–biotin complex ABC Kit (Vector Labs, Burlingame, CA, USA) counterstained with hematoxylin. Positive staining is visualized by the brown-colored (3,3-diaminobenzidine) (DAB) reaction product. The cross-reactivity of no. 3689 antibodies with porcine uPA was tested and confirmed first by performing a staining using kidney, an organ that is known to express uPA, from the same piglets (data not shown). Sections were also stained by H&E for histologic inspection by investigators masked to treatment.

Statistical Analysis

Pial artery diameter, CBF, CSF uPA, and MAPK isoform values were analyzed using analysis of variance for repeated measures. If the value was significant, the data were then analyzed by Fishers protected least significant difference test. An α level of $P < 0.05$ was considered significant in all statistical tests. Values are represented as mean ± s.e.m. of the absolute value or as percentage changes from control value.

Results

FPI Age Dependently Upregulates uPA and ERK MAPK in Cerebral Cortex and CSF

Figure 1 shows immunocytochemical and the corresponding histopathologic data derived from the same animals and areas of brain parenchyma, obtained from piglets 4 h after either FPI or sham control conditions. Abundant widespread uPA and phosphorylated (activated)-ERK MAPK staining in the parietal cortex of newborn-FPI-vehicle (0.9% saline) pigs was observed, primarily in association with neurons (Figures 1A and 1B). Neurons were identified by expression of NeuN (Figure 1C). ERK MAPK staining was substantially less prominent in newborn pigs treated with EEIIMD at the time of FPI, with staining for both antigens limited to the pia and a pial venule (Figures 1D and 1E). Little non-immune IgG activity is seen in a newborn-FPI-vehicle animal (Figure 1F), excluding nonspecific IgG binding. In contrast, minimal ERK MAPK and uPA staining was observed in neurons of juvenile pigs treated with vehicle at the time of FPI (Figures 1G and 1H). There was also minimal ERK MAPK and uPA staining restricted to pial venules (Figure 1J) and normal appearing neurons (Figure 1K) in juvenile pigs treated with EEIIMD at the time of FPI. There was little ERK MAPK and minimal uPA staining limited to the pia and pial vessels in sham control newborn animals (Figures 1M and 1N). H+ E staining showed normal appearing neurons/glia in sham newborns (Figure 1O), no obvious cortical damage in juvenile-FPI-vehicle animals (Figure 1I), but widespread cortical damage and hemorrhage in newborn-FPI-vehicle pigs (Figure 1L).

To estimate the amount of uPA detected in brain tissue, the concentration of uPA in cortical periarachnoid CSF was determined by enzyme-linked immunosorbent assay (ELISA). In the newborn, CSF uPA was increased within 1 min of FPI (Figure 2). In contrast, CSF uPA

concentration was not elevated at 1 min and only modestly elevated at 10 mins after insult in the juvenile (Figure 2). The concentration of uPA in the CSF was increased to a greater extent in newborn than juvenile pigs (Figure 2).

Total and phosphorylated ERK MAPK in cortical periarachnoid CSF was also measured by ELISA under baseline (before FPI, 0 time) and injury (1, 10, 60, and 240 mins) conditions. The activation (phosphorylation) state of this MAPK isoform was determined by expressing the data as a percent of control (total) to normalize these values. Vehicle (100 μL) alone (dimethylsulfoxide, diluted in 9.9 mL 0.9% saline) or antagonist was administered 30 mins before FPI. In the newborn, FPI induced a marked phosphorylation (activation) of CSF ERK MAPK within 1 min after injury (Figure 3A). ERK MAPK phosphorylation continued to increase in the CSF of newborns throughout the 4 h observation period (Figure 3A). In contrast, ERK MAPK phosphorylation was not increased at 1 min after FPI in the juvenile (Figure 3B). Within 10 mins of FPI, CSF ERK MAPK phosphorylation was increased in the juvenile, but values were significantly less in this age group at all time points compared with those measured in the newborn (Figures 3A and 3B). Pretreatment with the plasminogen activator inhibitor EEIIMD (1 mg/kg i.v.), blocked the phosphorylation of ERK MAPK at 1 min and blunted phosphorylation of ERK MAPK observed at subsequent time points after FPI in newborns (Figure 3A). Similarly, EEIIMD blunted ERK MAPK phosphorylation in the juvenile (Figure 3B). Pretreatment with the ERK MAPK inhibitor U 0126 (1 mg/kg i.v.) blocked FPI-induced ERK MAPK phosphorylation (Figures 3A and 3B). Exogenous administration of uPA to the cerebral cortex, in a concentration measured in CSF after FPI (Figure 2), further stimulated phosphorylation of ERK MAPK at 4 h after insult (Figure 3).

FPI Produces Cerebrovascular Hyperemia Through uPA, LRP, and ERK MAPK in an Age-Dependent Manner

Pial artery dilation was observed at 1 min after FPI in the newborn, but not in the juvenile pig (Figures 4A and 4B). Within 10 mins of injury, pial artery vasoconstriction was observed in both age groups, though the magnitude of this effect was greater in the newborn versus that in the juvenile (Figures 4A and 4B). EEIIMD (10^{-7} mol/L), suPAR (10^{-7} mol/L) and anti-LRP antibody (10 μg/mL) each blocked pial artery dilation observed at 1 min after FPI in the newborn (Figure 4A). Pial artery vasoconstriction observed at subsequent time points after FPI was blunted by EEIIMD, suPAR, and anti-LRP in both newborn and juvenile pigs (Figures 4A and 4B). In contrast, mouse IgG had no effect on FPI-induced changes in pial artery diameter (data not shown). U 0126 (10^{-6} mol/L) blunted the initial pial artery vasodilation in the newborn and also blunted the subsequent vasoconstriction at later time points in both the newborn and juvenile.

CBF in the cerebral cortex was increased within 1 min of FPI in the newborn but not in the juvenile pig (Figures 5A and 5B). Pretreatment with EEIIMD (1 mg/kg i.v.), suPAR (1 mg/kg i.v.), or anti-LRP antibody (0.1 mg/kg i.v.) 30 mins before insult blocked FPI-induced hyperemia (Figure 5A). At later time points, CBF was reduced both in the newborn and the juvenile, the magnitude of the decreases being greater in the former (Figure 5). Pretreatment with EEIIMD, suPAR, or anti-LRP blunted reductions in CBF after insult in both age groups, though the magnitude of such effect was greater in the newborn (Figure 5). Determinations of CBF were reproducible over time in sham control animals not subjected to injury (Figure 5).

EEIIIMD, suPAR, anti-LRP, IgG, and U 0126 Effects on Cerebral Hemodynamics in Sham Control Piglets

Administration of EEIIMD, suPAR, anti-LRP antibody, and U 0126 to the cerebral cortical surface had no effect on pial artery diameter. Similarly, intravenous administration of EEIIMD, suPAR, and U 0126 had no effect on CBF in sham control piglets.

Blood Chemistry

There were no statistical differences in blood chemistry between sham control, FPI, and FPI antagonist-treated newborn and juvenile animals before or after all experiments. For example, values of 7.46±0.05, 36±5, and 94±7 mmHg for pH, pCO_2, and pO_2, respectively, were obtained before FPI in newborn pigs, whereas comparable respective values of 7.44±0.06, 38±7, and 90±10 mmHg were obtained at 4 h after FPI. Mean arterial blood pressure was acutely increased within 1 to 3 mins of FPI in the juvenile (66±7 to 89±8 mmHg) whereas such values were decreased at 1 to 3 min in the newborn (65±6 to 50±5 mmHg), as previously published (Armstead and Kurth, 1994). At later time points (1 and 4 h after insult), mean arterial blood pressure was modestly reduced in newborns (65±6 to 58±4 mmHg), but not in juvenile pigs (Armstead and Kurth, 1994). The amplitude of the pressure pulse, used as an index of injury intensity, was equivalent in FPI-vehicle and FPI-antagonist animals in both newborn and juvenile pigs (1.9±0.1 atm).

Discussion

There are several important new findings in this study. First, immunohistochemical analysis showed the presence of uPA and phosphorylated (activated) ERK MAPK in piglet brain and their upregulation after FPI. Second, although it has been observed that plasminogen activator concentration was increased in the brain after focal cerebral ischemia (Hosomi *et al*, 2001), our studies are the first to show that uPA is upregulated after FPI. Both neurons and glia showed intense staining for uPA. These data cannot distinguish between the possibility that neurons/glia serve as the cellular site of origin for uPA and ERK MAPK or that uPA binds to these cells or both (e.g., to uPAR) after insult. However, these data do support the idea that uPA mediates ERK MAPK upregulation as there was considerably less phosphorylated ERK MAPK detected in FPI animals pretreated with EEIIMD which inhibits the signal transducing but not the proteolytic activity of plasminogen activators. Third, the robust staining for uPA and ERK MAPK in the newborn FPI piglet contrasted with the comparatively meager staining in the juvenile animals after FPI, supporting our concept of the age-dependent upregulation and relationship between both after insult. In a recent prior study (Armstead *et al*, 2006), we observed quantitatively less histopathology in newborn-FPI animals pretreated with EEIIMD. In this study, we similarly observed qualitatively less histopathology in newborn and juvenile brain injured pigs pretreated with EEIIMD. Importantly, we additionally observed qualitatively more histopathology in the newborn compared with the juvenile-FPI pig, which was correspondingly associated with more age-dependent staining for uPA and ERK MAPK. However, our present data do not provide a direct cause–effect relationship between cerebral hemodynamics and histopathology. Therefore, we acknowledge that an alternative hypothesis is that EEIIMD may afford protection against histopathology after FPI by as yet unidentified mechanisms independent of CBF.

Dysregulation of CBF is thought to contribute to the outcome after brain injury and its regulation often is a key consideration in clinical therapeutic strategies. We found that FPI produces an initial pial artery dilation and increase in CBF in the newborn at 1 min after insult. This observation confirms the earlier suggestion of early hyperemia after FPI in the newborn pig, as showed by near infrared spectroscopy (Armstead and Kurth, 1994).

Hyperemia in the newborn- FPI-vehicle animals was temporally associated with an increase in the CSF concentration of the phosphorylated (activated) form of ERK MAPK. EEIIMD blocked the phosphorylation of ERK MAPK and the initial hyperemia in the newborn-FPI animals. Topical administration of suPAR, which blocks uPA-mediated pial artery dilation (Armstead *et al*, 2005), and anti-LRP antibody also blocked pial artery dilation observed at 1 min after insult in the newborn pig. suPAR and anti-LRP antibody similarly blocked FPI-induced hyperemia in the newborn pig. In contrast, neither early hyperemia nor an increase in phosphorylated ERK MAPK in the CSF was observed in juvenile-FPI-vehicle animals. These data suggest that upregulation of uPA after FPI produces an age-dependent hyperemia through LRP and ERK MAPK.

TBI can cause flow-metabolism uncoupling, resulting in cerebral ischemia (CBF less than cerebral metabolic demand) or cerebral hyperemia (CBF in excess of cerebral metabolism) (Bruce *et al*, 1981; Richards *et al*, 2001). Reductions in CBF observed to occur early after TBI produces cerebral ischemia in clinical studies in adults (Coles, 2004). Decreased CBF and cerebral metabolism after TBI may not be problematic, however, if there is compensatory increased oxygen extraction (Diringer *et al*, 2002). After pediatric TBI, cerebral hypoperfusion appears to be the dominant derangement and is often associated with poor outcome (Vavilala *et al*, 2004; Adelson *et al*, 1997*a*; Coles, 2004). However, after severe TBI in children, CBF may actually be normal or high (Sharples *et al*, 1995) and result in cerebral hyperemia and hemorrhage.

Our studies should be interpreted in the context of several basic science models of brain injury in pediatric animals described previously. Adelson *et al* (1997*b*) described the motor and cognitive functional deficits using a weight drop model in the immature rat. Smith *et al* (1998) investigated the function of oxygen-free radicals in the sequelae of TBI using an infant rat model of the shaken baby syndrome. FPI is thought to be a good mimic of TBI in the pediatric population (Gennarelli, 1994). Prins *et al* (1996) compared the effects of FPI on mortality, intracranial pressure, and arterial blood pressure in the developing and adult rat. We have previously compared the cerebral hemodynamic effects of lateral FPI (2 atm, moderate injury) in newborn (1 to 5-day old) and juvenile (3 to 4-week old) pigs within the first 3 h of the insult (Armstead and Kurth, 1994). On the basis of interspecies extrapolation of brain growth curves (Dobbing, 1974), the age of the newborn pig roughly approximated the newborn–infant time period in the human, whereas the juvenile pig approximated that of an 8 to 10-year-old child. Marked differences in the effects of FPI in these two ages were observed: (1) we observed greater pial artery constriction and a greater and more protracted depression in CBF in newborn versus juvenile pigs, (2) there were marked increases in intracranial pressure in the newborn, but modest increases in the juvenile, (3) there were differences in the cerebral oxygenation, an index of metabolism—in the newborn saturation increased, followed by profound prolonged desaturation of hemoglobin for oxygen, while in the juvenile saturation increased modestly, followed by mild desaturation, (4) systemic arterial blood pressure increased in the juvenile but decreased in the newborn (Armstead and Kurth, 1994). These data indicate that cerebral and systemic hemodynamic responses after FPI are age dependent. However, the potential presence of an early hyperemia after insult has not been investigated to date.

This study is the first to our knowledge to show an age-dependent early hyperemia after FPI using equivalent levels of insult. The functional significance of this observation relates to hyperemic contributions to brain edema and neuronal cell death after TBI. Previously, endogenous plasminogen activators were observed to contribute to parietal cortex and hippocampal neuronal cell necrosis after FPI in the newborn pig (Armstead *et al*, 2006). The present studies extend these observations to show that age-dependent uPA upregulation after FPI contributes to distinctly different cerebral hemodynamic profiles in the two age

groupings of piglets. In turn, different hemodynamic profiles produce age-dependent histopathology that is dependent on the upregulation of ERK MAPK. As a consequence, the existence of a hyperemia predisposes towards a situation where there is an inability to discern whether outcome is more dependent on the traumatic insult itself or, more probably, due to TBI-induced secondary alterations in CBF. In this context, clinical intervention may be best directed to optimize CBF. Nonetheless, caution is urged in the interpretation of these results because how this force acts within the skull may well depend on differences in the composition and compliance of the newborn and juvenile pig brain itself in addition to the biochemical differences that we observed. In addition, it is unclear how developmental parameters such as brain water content, skull dimensions, or suture elasticity will affect the biomechanics of the fluid wave pulse delivered to the brains of these two age groups.

Clinically, it has been suggested that coagulopathy contributes to outcome in brain injury in the pediatric population (Hymel *et al*, 1997). tPA has been observed to contribute to excitotoxic neuronal cell death through activation of microglia or enhancement of NMDA receptor-mediated signaling (Nicole *et al*, 2001; Rogove *et al*, 1999; Tsirka *et al*, 1995). We have recently observed that the concentration of tPA in the CSF is elevated after FPI in an age-dependent manner (Armstead *et al*, 2005). In prior unrelated studies, FPI was observed to impair dilation in response to NMDA receptor activation in an age-dependent manner (Armstead, 2000). Because EEIIMD and suPAR partially prevented FPI-induced impairment of NMDA-mediated cerebrovasodilation, plasminogen activators contribute to the age-dependent impairment of NMDA cerebrovasodilation after brain injury (Armstead *et al*, 2005). Because EEIIMD and suPAR also partially prevented pial artery vasoconstriction after injury in an age-dependent manner, we inferred that endogenous plasminogen activators contribute to altered cerebral hemodynamics after FPI (Armstead *et al*, 2005). This study supports and extends these observations using biochemical, pharmacologic, and immunohistochemical approaches by showing the function of uPA in regulating both CBF as well as pial artery diameter after insult.

In conclusion, results of this study show that uPA is upregulated after FPI and produces an age-dependent early hyperemia in an LRP- and ERK MAPK-dependent pathway that is associated with greater histopathology in the newborn. These data suggest that the endogenous plasminogen activator system contributes to outcome after TBI in an age-dependent manner.

Acknowledgments

This research was supported by grants from the National Institutes of Health, NS53410 and HD57355 (WMA), HL76406, CA83121, HL76206, HL07971, and HL81864 (DBC), HL77760 and HL82545 (AARH), the University of Pennsylvania Research Foundation (WMA), the University of Pennsylvania Institute for Translational Medicine and Therapeutics (DBC), and the Israeli Science Foundation (AARH).

References

Adelson PD, Clyde B, Kochanek PM, Wisniewski SR, Marion DW, Yonas H. Cerebrovascular response in infants and young children following severe traumatic brain injury: a preliminary report. Pediatr Neurosurg. 1997a; 26:200–7. [PubMed: 9436831]

Adelson PD, Dixon CE, Robichaud P, Kochanek PM. Motor and cognitive functional deficits following diffuse traumatic brain injury in the immature rat. J Neurotrauma. 1997b; 14:99–108. [PubMed: 9069441]

Akkawi S, Nassar T, Tarshis M, Cines DB, Higazi AAR. LRP and avB3 mediate tPA-activation of smooth muscle cells. AJP. 2006; 291:H1351–9.

Armstead WM. NOC/oFQ contributes to age dependent impairment of NMDA induced cerebrovasodilation after brain injury. Am J Physiol. 2000; 279:H2188–95.

Armstead WM. PTK, ERK, and p38 MAPK contribute to impaired NMDA vasodilation after brain injury. Eur J Pharmacol. 2003; 474:249–54. [PubMed: 12921870]

Armstead WM, Cines DB, Higazi AAR. Plasminogen activators contribute to age dependent impairment of NMDA cerebrovasodilation after brain injury. Dev Brain Res. 2005; 156:139–46. [PubMed: 16099300]

Armstead WM, Kurth CD. Different cerebral hemodynamic responses following fluid percussion brain injury in the newborn and juvenile pig. J Neurotrauma. 1994; 11:487–97. [PubMed: 7861442]

Armstead WM, Nassar T, Akkawi S, Smith DH, Chen XH, Cines DB, Higazi AAR. Neutralizing the neurotoxic effects of exogenous and endogenous tPA. Nat Neurosci. 2006; 9:1150–7. [PubMed: 16936723]

Bonni A, Brunet A, West AE, Datta SR, Takasu MA, Greenberg ME. Cell survival promoted by the Ras-MAPK signaling pathway by transcription-dependent and -independent mechanisms. Science. 1999; 286:1358–62. [PubMed: 10558990]

Bruce DA, Alavi A, Bilaniuk L, Dolinskas C, Obrist W, Uzzell B. Diffuse cerebral swelling following head injuries in children; the syndrome of malignant brain edema. J Neurosurg. 1981; 54:170–8. [PubMed: 7452330]

Bu G, Wjilliams S, Strickland DR, Schwartz AL. Low density lipoprotein receptor-related protein/alpha 2-macroglobulin receptor is an hepatic receptor for tissue-type plasminogen activator. PNAS. 1992; 89:7427–31. [PubMed: 1502154]

Coles JP. Regional ischemia after head injury. Curr Opin Crit Care. 2004; 10:120–5. [PubMed: 15075722]

Collen D, Lijnen HR. Basic and clinical aspects of fibrinolysis and thrombolysis. Blood. 1991; 78:3114–24. [PubMed: 1742478]

Diringer MN, Videen TO, Yundt K, Zazulia AR, Aiyagari V, Dacey RG Jr, Grubb RL, Powers WJ. Regional cerebrovascular and metabolic effects of hyperventilation after severe traumatic brain injury. J Neurosurg. 2002; 96:103–8. [PubMed: 11794590]

Dobbing J. The later growth of the brain and its vulnerability. Pediatrics. 1974; 53:2–6. [PubMed: 4588131]

Gennarelli TA. Animate models of human head injury. J Neurotrauma. 1994; 11:357–68. [PubMed: 7837277]

Hicks RR, Martin VB, Zhang L, Seroogy KB. Mild experimental brain injury differentially alters the expression of neurotrophin and neurotrophin receptor mRNAs in the hippocampus. Exp Neurol. 1999; 160:469–78. [PubMed: 10619564]

Higazi AA, Bdeir K, Hiss E, Arad S, Kuo A, Barghouti C, Cines DB. Lysis of plasma clots by urokinase-soluble urokinase receptor complexes. Blood. 1998; 92:2075–83. [PubMed: 9731065]

Higazi AA, Mazar A, Wang J, Reilly R, Henkin J, Kniss D, Cines D. Single chainurokinase-type plasminogen activator bound to its receptor is relatively resistant to plasminogen activator inhibitor type 1. Blood. 1996a; 87:3545–9. [PubMed: 8611676]

Higazi AA, Upson RH, Cohen RL, Manuppello J, Bognacki J, Henkin J, McCrae KR, Kounnas MZ, Strickland DK, Preissner KT, Lawler J, Cines DB. Interaction of single-chain urokinase with its receptor induces the appearance and disappearance of binding epitopes within the resultant complex for other cell surface proteins. Blood. 1996b; 88:542–51. [PubMed: 8695802]

Hosomi N, Jucero J, Heo JH, Koziol JA, Copeland BR, del Zoppo GJ. Rapid differential endogenous plasminogen activator expression after acute middle cerebral artery occlusion. Stroke. 2001; 32:1341–8. [PubMed: 11387497]

Hymel KP, Abshire TC, Luckey DW, Jenny C. Coagulopathy in pediatric abusive head trauma. Pediatrics. 1997; 99:371–5. [PubMed: 9041291]

Laher I, Zhang JH. Protein kinase C and cerebral vasospasm. J Cereb Blood Flow Metab. 2001; 21:887–906. [PubMed: 11487724]

Leffler CW, Busija DW, Mirro R, Armstead WM. Effects of ischemia on brain blood flow and oxygen consumption of newborn pigs. Am J Physiol. 1989; 257:H1917–26. [PubMed: 2513731]

Nassar T, Akkawi S, Shin A, Haj-Yehia A, Bdeir K, Tarshis M, Heyman SN, Higazi AA. *In vitro* and *in vivo* effects of tPA and PAI-1 on blood vessel tone. Blood. 2004; 103:897–902. [PubMed: 14512309]

Nassar T, Haj-Yehia A, Akkawi S, Kuo A, Bdeir K, Mazar A, Cines DB, Higazi AA. Binding of urokinase to low density lipoprotein-related receptor (LRP) regulates vascular smooth muscle cell contraction. J Biol Chem. 2002; 277:40499–504. [PubMed: 12171938]

Nicole O, Docagne F, Ali C, Margaill I, Carmeliet P, MacKenzie ET, Vivien D, Buisson A. The proteolytic activity of tissue-plasminogen activator enhances NMDA receptor-mediated signaling. Nat Med. 2001; 7:59–64. [PubMed: 11135617]

Otani N, Nawashiro H, Fukui S, Nomura N, Shima K. Temporal and spatial profile of phosphorylated mitogen-activated protein kinase pathways after lateral fluid percussion injury in the cortex of the rat brain. J Neurotrauma. 2002; 19:1587–96. [PubMed: 12542859]

Prins ML, Lee SM, Cheng CL, Becker DP, Hovda DA. Fluid percussion brain injury in the developing and adult rat: a comparative study of mortality, morphology, intracranial pressure and mean arterial blood pressure. Brain Res Dev Brain Res. 1996; 95:272–82.

Richards HK, Simac S, Piechnik S, Pickard JD. Uncoupling of cerebral blood flow and metabolism after cerebral contusion in the rat. J Cereb Blood Flow Metab. 2001; 21:779–81. [PubMed: 11435789]

Rodriguez JG. Childhood injuries in the United States. A priority issue. Am J Dis Child. 1990; 144:625–6. [PubMed: 2346145]

Rogove AD, Siao C, Keyt B, Strickland S, Tsirka SE. Activation of microglia reveals a non-proteolytic cytokine function for tissue plasminogen activator in the central nervous system. J Cell Sci. 1999; 112:4007–16. [PubMed: 10547361]

Sharples PM, Stuart AG, Matthews DS, Aynsley-Green A, Eyre JA. Cerebral blood flow and metabolism in children with severe head injury. Part I: relation to age, Glasgow coma score, outcome, intracranial pressure, and time after injury. J Neurol Neurosurg Psychiatry. 1995; 58:145–52. [PubMed: 7876842]

Smith SL, Andrus PK, Gleason DD, Hall ED. Infant rat model of the shaken baby syndrome: preliminary characterization and evidence for the role of free radicals in cortical hemorrhaging and progressive neuronal degeneration. J Neurotrauma. 1998; 15:693–705. [PubMed: 9753217]

Tsirka SE, Gualandris A, Amaral DG, Strickland S. Excitotoxin-induced neuronal degeneration and seizure are mediated by tissue plasminogen activator. Nature. 1995; 377:340–4. [PubMed: 7566088]

Vavilala MS, Lee LA, Boddu K, Visco E, Newell DW, Zimmerman JJ, Lam AM. Cerebral autoregulation in pediatric traumatic brain injury. Pediatr Crit Care Med. 2004; 5:257–63. [PubMed: 15115564]

Wei EP, Dietrich WD, Povlishock JT, Navari RM, Kontos HA. Functional, morphological, and metabolic abnormalities of the cerebral microcirculation after concussive brain injury in cats. Circ Res. 1980; 46:37–47. [PubMed: 7349916]

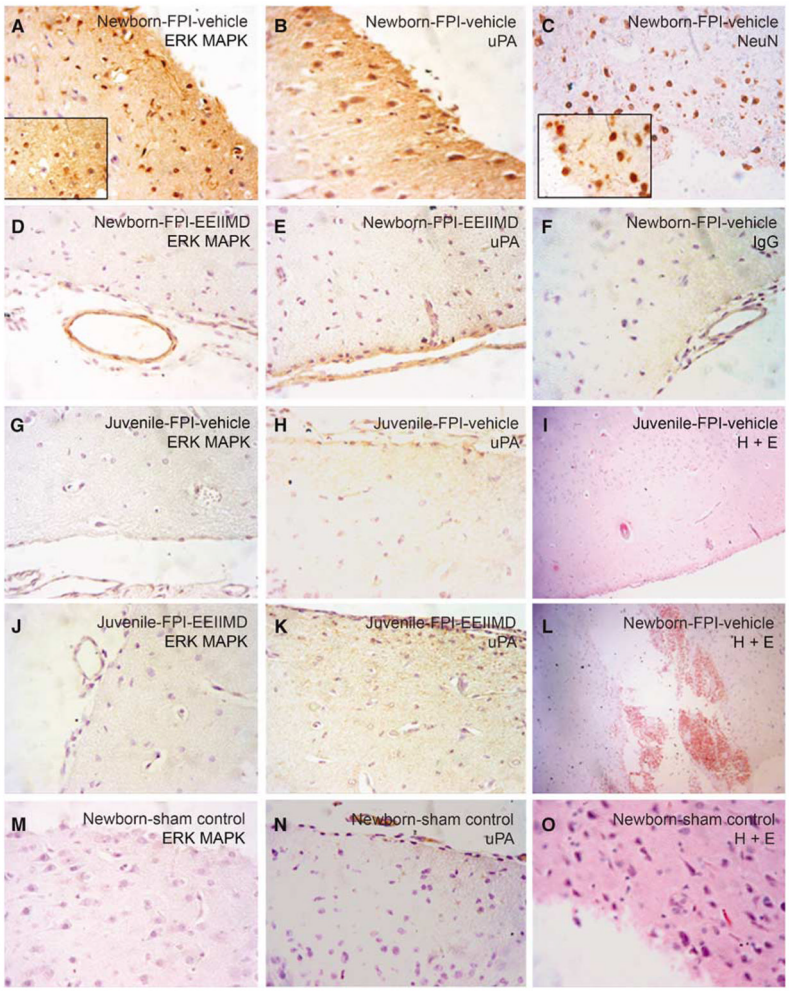

Figure 1.

Immunohistochemistry and histopathology 4 h after FPI. Sections of the parietal cortex from piglet brains after FPI (**A**–**C**, **F**, **L**, newborn vehicle; **D**, **E**, newborn-EEIIMD 1 mg/kg i.v.; **G**–**I**, juvenile-vehicle; **J**, **K**, juvenile-EEIIMD) and from uninjured control animal (**M**–**O**, newborn vehicle), were subjected to antigen retrieval in citrate buffer and stained with anti-phospho-ERK rabbit monoclonal antibody (2 μg/mL) (no. 4376; Cell Signaling) (**A**, **D**, **G**, **J**, **M**), or with anti-uPA monoclonal antibody (5 μg/mL) (no. 3689; American Diagnostica) (**B**, **E**, **H**, **K**, **N**), with mouse anti-neuronal nuclei monoclonal antibody (5 μg/mL) as a neuronal marker (no. MAB377; Chemicon International, Billerica, MA, USA) (**C**), or with nonimmune mouse IgG_1 as a negative control (**F**), secondary biotinylated anti-mouse IgG (1:200), followed by incubation with HRP-conjugated streptavidin. Magnification shown is ×400 for all panels except (**I**, **L)** which was ×100 and ×1,000 for inserts in (**A**, **C**). Adjacent sections from the same brains exposed to brain injury (**I**, **L**) and from uninjured control (**O**), were stained by H&E for histologic inspection. These data reflect an *n* of 2 per experimental group.

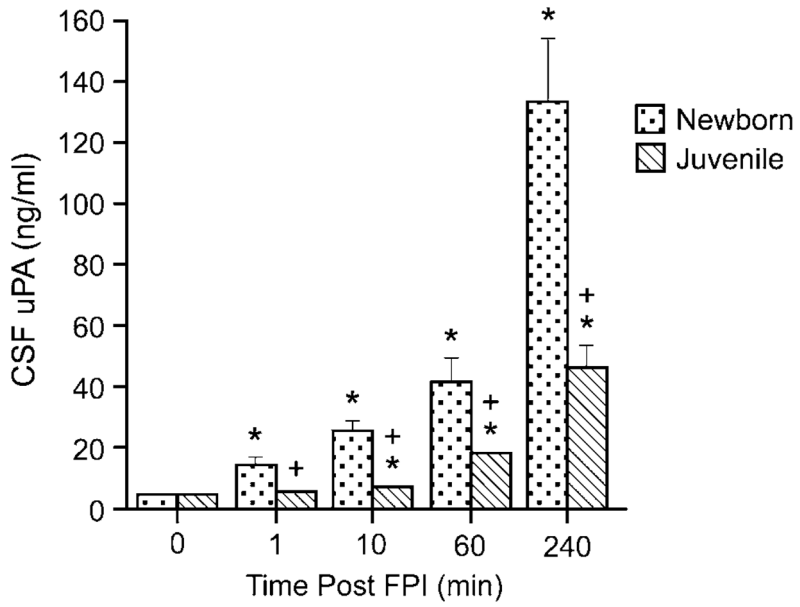

Figure 2.

Influence of FPI on CSF uPA concentration (ng/mL) as a function of time after insult (min) in newborn and juvenile pigs, n=6. *P<0.05 versus corresponding pre-FPI (0 time) value $^{+}$ P<0.05 versus corresponding newborn value.

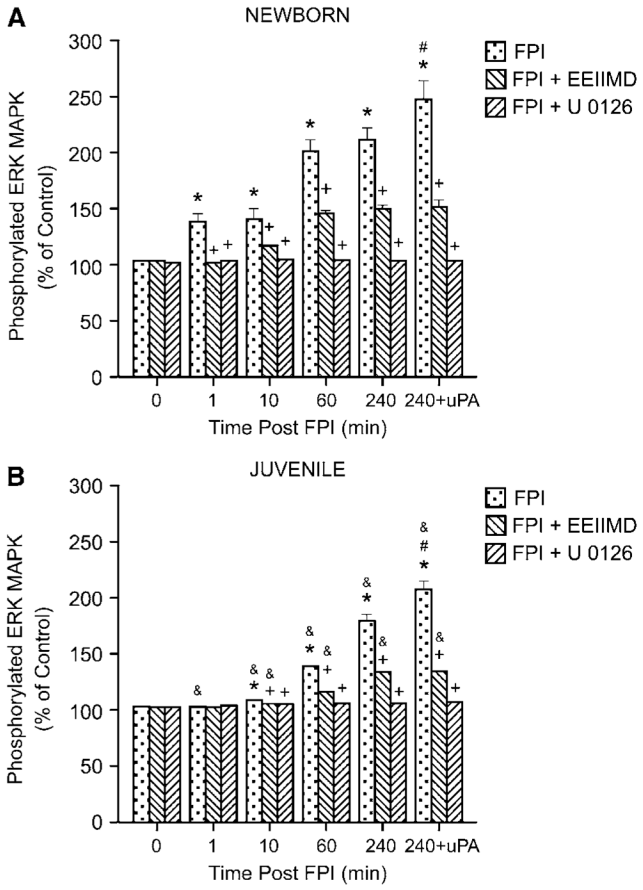

Figure 3.

Phosphorylation of ERK MAPK in cortical periarachnoid CSF before FPI (0 mins), as a function of time (min) after FPI, and 4 h after FPI and additional exogenous administration of uPA (10^{-7} mol/L) in vehicle (FPI), EEIIMD (1 mg/kg i.v.)+ FPI, and U 0126 (1 mg/kg i.v.)+FPI animals, n=6. Data expressed as percentage of control by ELISA determination of phospho-MAPK and total MAPK isoforms and subsequent normalization to total form. (**A**) Newborn, (**B**) juvenile. *P<0.05 compared with corresponding 0 time value. ^{+}P<0.05 compared with corresponding FPI non-pretreated value. $^{\#}P$<0.05 compared with corresponding 240 mins non-uPA-treated value. $^{\&}P$<0.05 compared with corresponding newborn value.

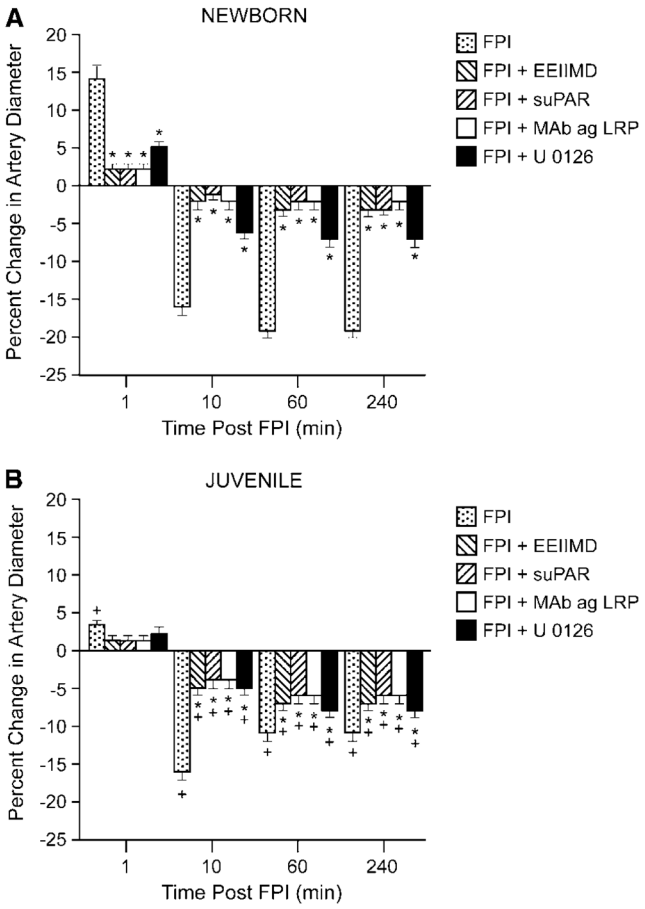

Figure 4.

Influence of FPI on pial artery diameter in the absence and presence of EEIIMD (10^{-7} mol/L), suPAR (10^{-7} mol/L), anti-LRP antibody (Mab ag LRP, 10 μg/mL), and U 0126 (10^{-6} mol/L) pretreatment 30 mins before injury, n=6. (**A**) Newborn, (**B**) juvenile. *P<0.05 compared with corresponding FPI-alone value. ^{+}P<0.05 compared with corresponding value in the newborn.

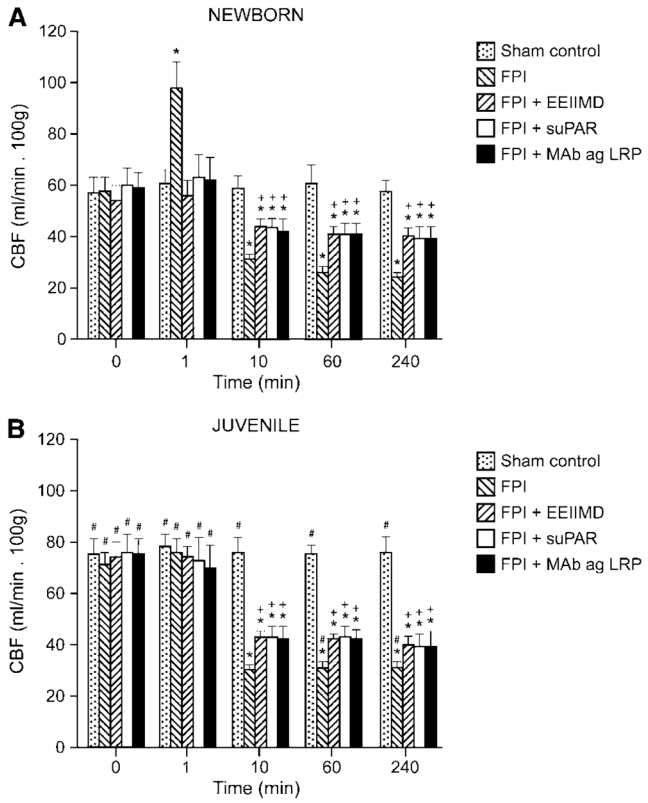

Figure 5.

Blood flow in the cerebral cortex (CBF) in sham control, FPI, FPI+EEIIMD (1 mg/kg i.v.), FPI+suPAR (1 mg/kg i.v.), and FPI+anti-LRP antibody (0.1 mg/kg i.v.), 30 mins pretreatment animals, n=3 to 4. (**A**) newborn, (**B**) juvenile. *P<0.05 compared with corresponding sham control value. ^{+}P<0.05 compared with corresponding FPI non-pretreated value. $^{\#}P$<0.05 compared with corresponding newborn value.